

AD-A041 239

AEROSPACE CORP EL SEGUNDO CALIF IVAN A GETTING LABS F/G 4/1
NEUTRAL ATMOSPHERIC WAVES IN THE THERMOSPHERE AND TROPOSPHERIC --ETC(U)
MAY 77 C J RICE, L R SHARP F04701-76-C-0077

UNCLASSIFIED

TR-0077(2960-04)-3

SAMSO-TR-77-98

NL

1 OF 1
ADAO41239



AD A 041 239

Neutral Atmospheric Waves in the Thermosphere and Tropospheric Weather Systems

Space Sciences Laboratory
The Ivan A. Getting Laboratories
The Aerospace Corporation
El Segundo, Calif. 90245

10 May 1977

Interim Report

APPROVED FOR PUBLIC RELEASE:
DISTRIBUTION UNLIMITED

DDC
RECEIVED
JUL 5 1977
C

Prepared by
SPACE AND MISSILE SYSTEMS ORGANIZATION
AIR FORCE SYSTEMS COMMAND
Los Angeles Air Force Station
P.O. Box 92960, Worldway Postal Center
Los Angeles, Calif. 90009

AD No.

DDC FILE COPY

This interim report was submitted by The Aerospace Corporation, El Segundo, CA 90245, under Contract No. F04701-76-C-0077 with the Space and Missile Systems Organization, Deputy for Advanced Space Programs, P.O. Box 92960, Worldway Postal Center, Los Angeles, CA 90009. It was reviewed and approved for The Aerospace Corporation by G. A. Paulikas, Director, Space Sciences Laboratory. Lieutenant Dara Batki, SAMSO/YAPT, was the project officer for Advanced Space Programs.

This report has been reviewed by the Information Office (OI) and is releasable to the National Technical Information Service (NTIS). At NTIS, it will be available to the general public, including foreign nations.

This technical report has been reviewed and is approved for publication.

FOR THE COMMANDER

Dara Batki

Dara Batki, Lt, USAF
Project Officer

Joseph Gassmann
Joseph Gassmann, Major, USAF

Floyd R. Stuart
Floyd R. Stuart, Colonel, USAF
Deputy for Advanced Space Programs

ACCESSION FOR	NTIS	NTIS Section	<input checked="checked" type="checkbox"/>
	DTIC	DTIC Section	<input type="checkbox"/>
	UNCLASSIFIED		
	RESTRICTED		
BY DISTRIBUTION/AVAILABILITY CODES			
Dist.	APPL. and/or SPECIAL		
R			

UNCLASSIFIED

SECURITY CLASSIFICATION OF THIS PAGE (When Data Entered)

19 REPORT DOCUMENTATION PAGE		READ INSTRUCTIONS BEFORE COMPLETING FORM
1. REPORT NUMBER SAMSØ-TR-77-98	2. GOVT ACCESSION NO.	3. RECIPIENT'S CATALOG NUMBER
4. TITLE (and Subtitle) NEUTRAL ATMOSPHERIC WAVES IN THE THERMOSPHERE AND TROPOSPHERIC WEATHER SYSTEMS.	5. TYPE OF REPORT & PERIOD COVERED Interim	6. PERFORMING ORG. REPORT NUMBER TR-0077(2960-04)-3
7. AUTHOR(s) Carl J. Rice and Lawrence R. Sharp	8. CONTRACT OR GRANT NUMBER(s) F04701-76-C-0077	9. PROGRAM ELEMENT, PROJECT, TASK AREA & WORK UNIT NUMBERS 12/28p.
10. CONTROLLING OFFICE NAME AND ADDRESS Space and Missile Systems Organization Air Force Systems Command Los Angeles, Calif. 90009	11. REPORT DATE 10 May 1977	12. NUMBER OF PAGES 24
13. MONITORING AGENCY NAME & ADDRESS (if different from Controlling Office)	14. SECURITY CLASS. (of this report) Unclassified	15a. DECLASSIFICATION/DOWNGRADING SCHEDULE
16. DISTRIBUTION STATEMENT (of this Report) Approved for public release; distribution unlimited.		
17. DISTRIBUTION STATEMENT (of the abstract entered in Block 20, if different from Report)		
18. SUPPLEMENTARY NOTES		
19. KEY WORDS (Continue on reverse side if necessary and identify by block number) Upper Atmosphere Neutral Thermosphere Internal Atmospheric Gravity Waves Thermospheric-Tropospheric Interaction		
20. ABSTRACT (Continue on reverse side if necessary and identify by block number) Neutral atmospheric density profiles between 130 and 225 km obtained by a cold cathode ion gauge onboard the AE-C spacecraft frequently exhibit considerable wave-like structure. This structure is interpreted to be propagating internal gravity waves. We have attempted to correlate the probability of occurrence and amplitude of the waves with several parameters of geophysical importance. Only weak or no correlation is found with the common parameters, such as Kp, for which a dependence of the average total density		

DD FORM 1473
(FACSIMILE)

UNCLASSIFIED

SECURITY CLASSIFICATION OF THIS PAGE (When Data Entered)

409 944

next page

UNCLASSIFIED

SECURITY CLASSIFICATION OF THIS PAGE(When Data Entered)

19. KEY WORDS (Continued)

20. ABSTRACT (Continued)

cont → is known to exist. The waves do seem to appear in certain preferred geographical locations, however. These locations tend to coincide with regions of high wind speeds in the upper troposphere. This leads us to suggest that the majority of the observed waves originate in the troposphere, subsequently propagating upwards into the thermosphere.

↑

UNCLASSIFIED

SECURITY CLASSIFICATION OF THIS PAGE(When Data Entered)

PREFACE

We would like to thank Ms. Judy Palmer and Ms. Vera J. Bledsoe for their efforts in the data reduction. We have profited from many valuable discussions with Dr. D. R. Hickman, Dr. Y. T. Chiu, Dr. J. M. Straus, and Ms. B. K. Ching.

REDUCTION for	
NTIS	Write Section <input checked="" type="checkbox"/>
DDC	Buff Section <input type="checkbox"/>
UNANNOUNCED	<input type="checkbox"/>
JUSTIFICATION	
BY	
DISTRIBUTION/AVAILABILITY CODES	
Dist.	Avail. and/or SPECIAL
A	

CONTENTS

PREFACE	1
INTRODUCTION	7
DATA PRESENTATION	9
DISCUSSION	20
REFERENCES	27

FIGURES

1.	Atmospheric Neutral Density (g/cm^3) Vs. Altitude (km) Profile From the PSA Instrument for AE-C in the Despun Mode	8
2.	Percentage of Data Points at Each of the Discrete Altitudes Which Falls Into Each of the Four Wave Classification Categories	11
3.	Percentage of Data Points Which Fall Into Each Wave Classification as a Function of Simultaneous Kp Index and the Kp Index 6 Hours Prior to the Measurements	12
4.	Average Neutral Density Vs. Altitude Profiles Obtained by Dividing All Data According to the Local Wave Classification and Averaging at Each Altitude	13
5.	Average Neutral Density Vs. Altitude Profile Obtained as for Figure 4 Except That Data Division Is According to a 4-Step Disturbance Index Which Characterizes the State of Agitation of a Full Upleg or Downleg Portion of a Pass	14
6.	Orbital Parameters for AE-C Encompassing the Period of Operation in the Elliptic Phase	16
7.	Percentage Frequency of Occurrence of Each Wave Classification as a Function of Local Time	17
8.	Percentage Frequency of Occurrence of Each Wave Classification as a Function of Geographic Latitude	18
9.	Contours Showing Percentage Frequency of Occurrence of Wave Classifications 3 and 4 as a Function of Latitude (10° Bins) and Longitude (30° Bins)	19
10.	Same as Figure 9 Except That Data Base Has Been Divided Into Halves by a Random Selection of Orbits	21
11.	Location of the Mean Sub-Tropical Jet Stream During the Winter of 1955-56	22
12.	Profiles of Average Mid-Season Zonal Winds at 500 mb in the Northern and Southern Hemispheres	24
13.	Mean Winds at 200 mb in January and July	25

INTRODUCTION

A satellite which operates within the sensible atmosphere is subject to drag effects which modify the satellite's orbit. In order to predict such effects, model neutral atmospheres have been developed and incorporated into ephemeris prediction routines. New models continue to appear, but even though the new models may be satisfying from a scientific point of view, incorporating new physical insights in a more explicit or self-consistent fashion, it is well known within the community of developers and users of these empirical models that little progress has been made in the last decade in improving their operational (i.e., predictive) capabilities. For example, the Air Force Satellite Control Facility uses a model which is more than 15 years old for operational ephemeris prediction and control of low altitude spacecraft; the Aerospace Defense Command uses a model developed by Jacchia in 1964. Despite the best efforts of many people, all models developed and tested since the mid-sixties do not give sufficiently better operational performance to justify the costs which would be incurred in changing to more recently developed models. In all such models, either of recent or of ancient vintage, using simple approximate mathematical expressions or complex "exact" integrations, there appear to be residual errors on the order of 10-15%. These errors exist and are inevitable because unmodeled residuals of the same magnitude exist within the data base used in developing the models themselves (see, for example, the accuracy analyses which appear in the CIRA 1965, CIRA 1972, OGO-6 (Hedin et al., 1974), and MSIS (Hedin et al., 1977a,b) models.

Neutral density data derived from sensors flown on the NASA Atmosphere Explorer (AE) satellites lead us to conclude that at least part of the source of the 10-15% residuals is due to the presence of wave-like turbulence in the upper atmosphere. Structure such as that seen in Figure 1 is commonly encountered during perigee passes of the AE satellites. Our studies presented here indicate that the presence and amplitude of such structure correlates only weakly or not at all with parameters such as $F_{10.7}$, Kp, local time, etc., which are used to model the neutral density. In a more direct sense, there appears to be no significant correlation between the magnitude of the local neutral density and the presence or absence of waves. Nevertheless, such structure will alter the drag force experienced by the satellite during a specific orbit depending on the amplitude

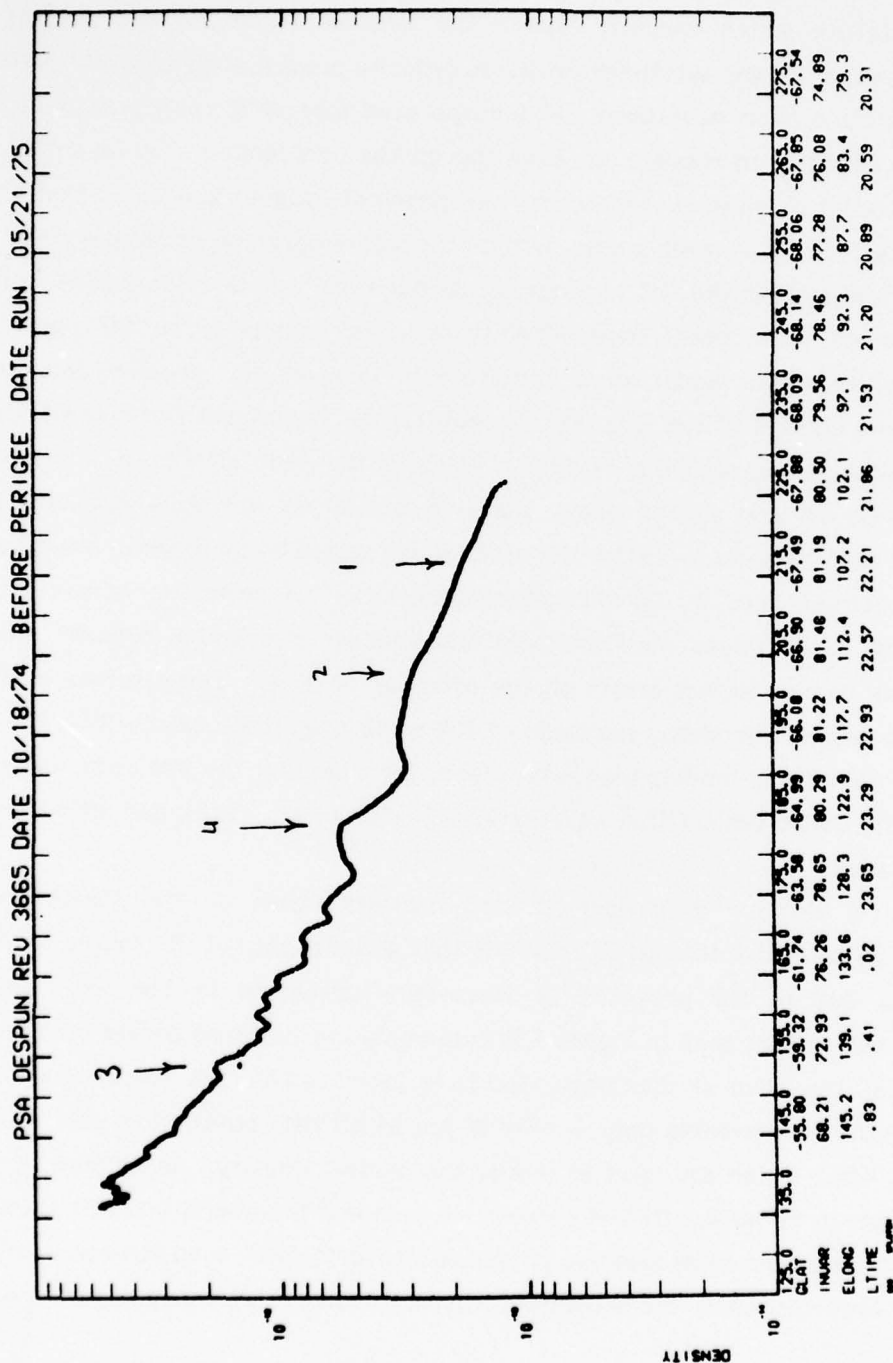


Figure 1. Atmospheric neutral density (g/cm^3) vs. altitude (km) profile from the PSA instrument for AE-C in the despun mode. The numbered segments illustrate the examples which fall in each of the four classifications of the "wave" or "bump" index (see text).

and phase of any waves encountered near perigee. On the other hand, the data do have certain geographic regularities in the occurrence of these wave structures which are similar to the global distribution of high velocity jet stream winds in the upper troposphere.

When Colin Hines first proposed that certain motions in the upper atmosphere might be interpreted as propagating internal atmospheric gravity waves, (Hines, 1960), he also suggested some candidates for the origin of such waves. Broadly speaking, these possible candidates can be divided into two groups: first, those whose source lies within the thermosphere itself, such as precipitating particles, substorms, aurorae, electrojet activity, etc.; and second, those whose actual source lies within the lower atmosphere, such as tropospheric wind systems, with some fraction of their energy leaking upwards into the thermosphere. While ground-based observers of the ionosphere have often attributed the origin of observed ionospheric waves to storm systems and other tropospheric phenomena, experimenters observing the neutral atmosphere with satellite-borne instruments have tended to favor the high altitude sources, often to the total exclusion of possible tropospheric sources from consideration. We feel that the geographic regularities seen in AE neutral density data support a tropospheric source for the majority of the observed thermospheric waves.

DATA PRESENTATION

Figure 1 shows an example of a neutral density vs. altitude profile obtained with a cold cathode gauge, which is known as Pressure Sensor A, or PSA, while AE-C was in a despun condition. The instrument is described in detail in Rice, et al. (1973). In order to build a manageable data base we have taken profiles such as this and concentrated on certain fixed altitude levels between 135 and 225 km, storing density and ephemeris data and, in addition, an index from 1 to 4 which characterizes the level of wave activity within a narrow altitude band. This index, illustrated in Figure 1, specifies the structure as follows:

- 1 : indicates a smoothly varying profile;
- 2 : indicates minor fluctuations, up to 5% amplitude;
- 3 : indicates the presence of waves between 5% and 15% amplitude;
- 4 : indicates pronounced waves with amplitudes greater than 15%.

For many purposes, we combine classes 3 and 4 for use as an indication of the presence of unambiguous wave activity. Utilizing a data base consisting of more than 5500 individual points from more than 300 orbits we have looked for regularities in the occurrence of these waves; the data base encompasses the period of the elliptic phase of AE-C from launch in December 1973 to circularization of the orbit in December 1974.

In Figure 2 are plotted the percentage of passes through each altitude bin which fall into each of the 4 wave classifications. The trend is clearly toward increasing wave activity with decreasing altitude. The deviation at 135 km may be real but is more likely an artifact caused by the fact that the satellite just skimmed this altitude in most cases. There is also an apparent tendency for waves at higher altitude to have longer wavelengths implying that the shorter wavelengths are being dissipated at lower altitudes. In subsequent graphs (except Figures 4 and 5) the data for 135 km and for 225 km are not included.

We have looked for correlations of wave activity with the Kp index with the results shown in Figure 3 for the simultaneous value of Kp and for Kp delayed by six hours. It appears that the Kp dependence is at most weak although there may be a slight increase in the occurrence of waves for Kp values of 5 or higher.

The altitude vs. neutral density profiles shown in Figure 4 were derived by dividing the data base according to the local wave index value and then determining the average density at each altitude. There are only slight separations between the 4 profiles derived in this way and certainly no systematic variations. In Figure 5 are similar profiles derived in this case by using a 4-step index which characterizes the general state of agitation for the complete upleg or downleg. Utilizing this index does not separately bin values derived from adjacent altitudes on a given pass. As with Figure 4, however, the profiles almost precisely overlap one another. Thus, except for the unlikely possibility of compensating effects, the presence or absence of the waves seems to be independent of

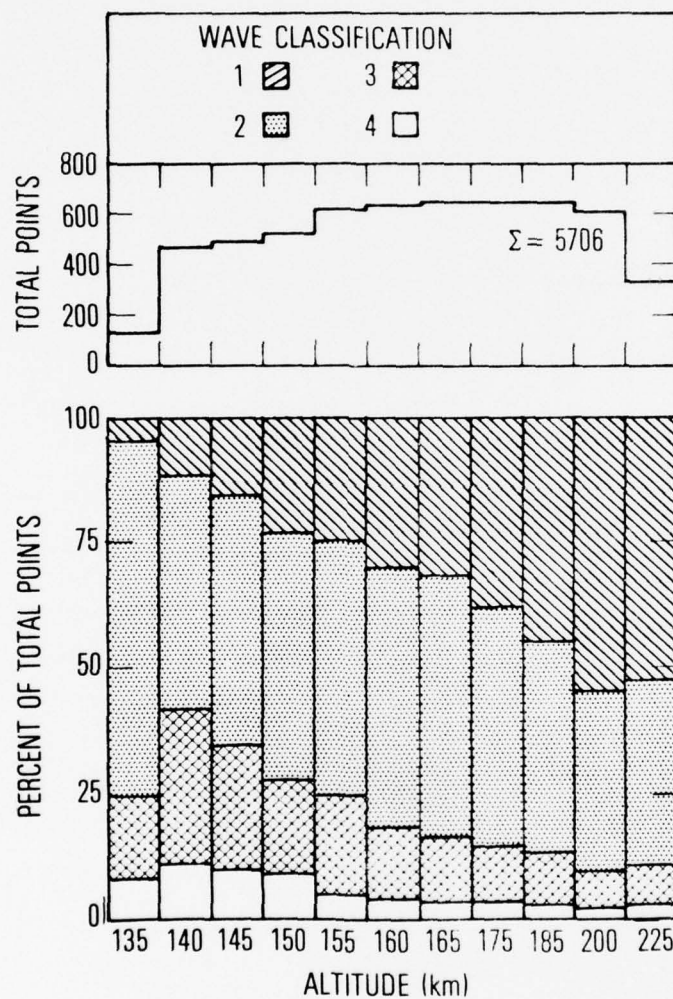


Figure 2.

Percentage of data points at each of the discrete altitudes which falls into each of the four wave classification categories. The total number of points in each altitude bin is given at the top.

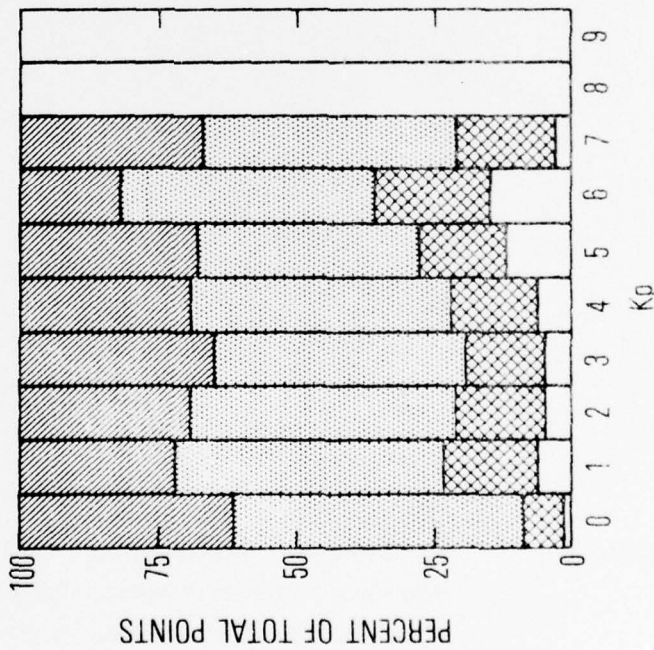
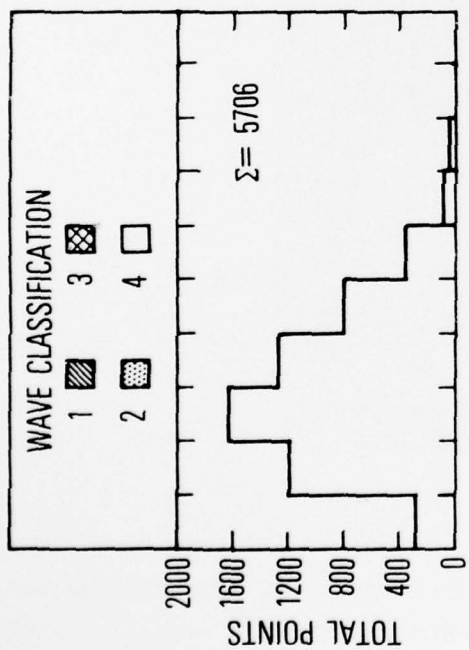
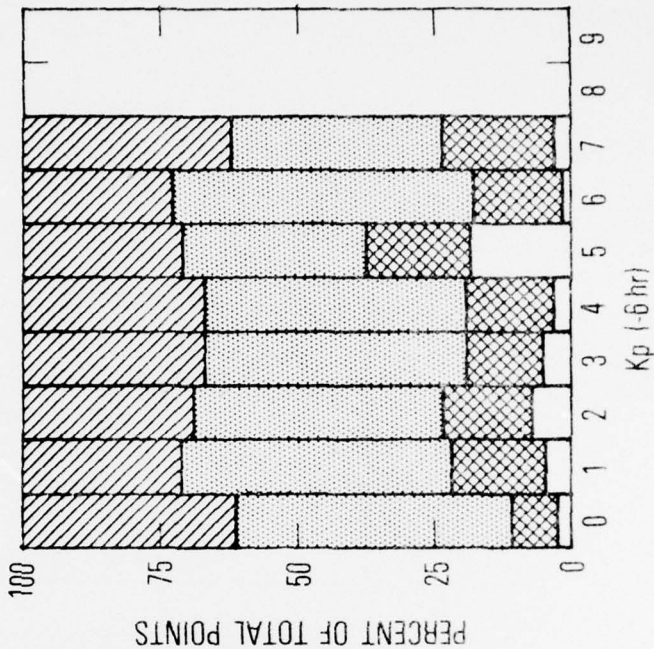
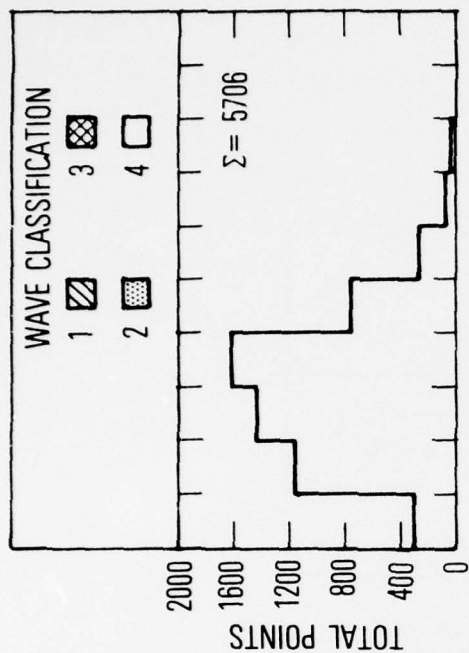


Figure 3. Percentage of data points which fall into each wave classification as a function of (A.) simultaneous Kp index and (B.) the Kp index 6 hours prior to the measurement.

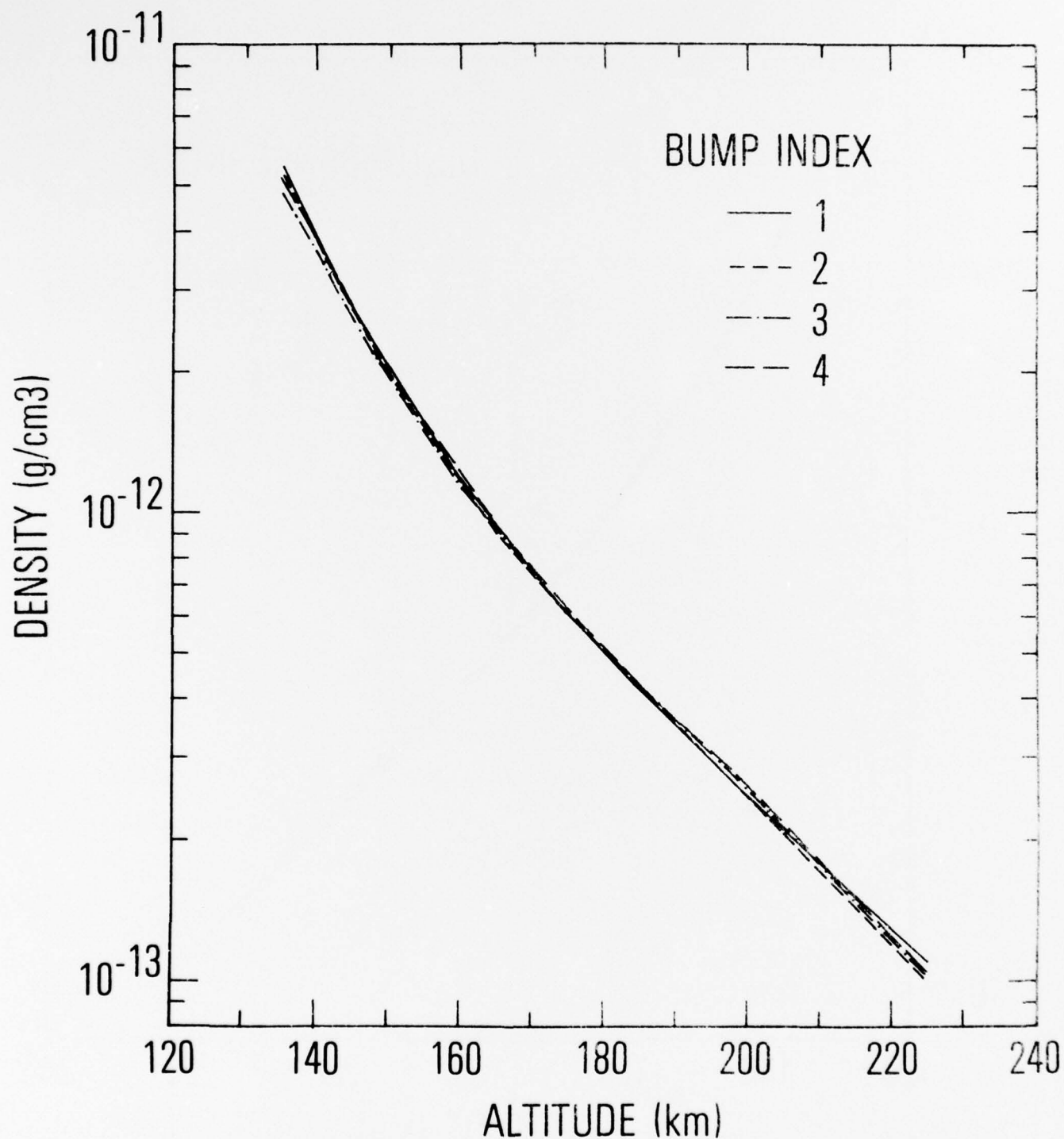


Figure 4.

Average neutral density vs. altitude profiles obtained by dividing all data according to the local wave classification and averaging at each altitude.

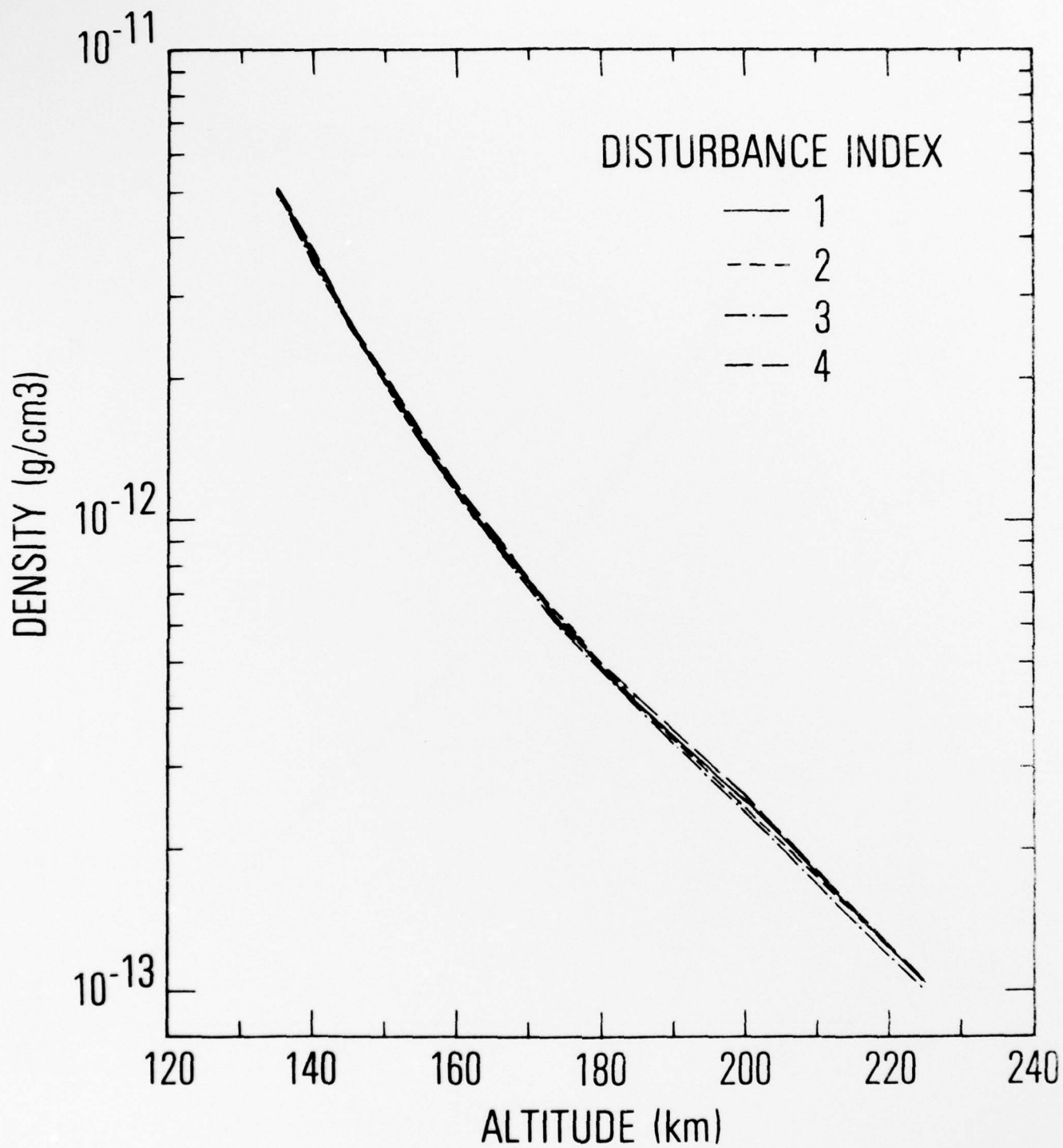


Figure 5. Average neutral density vs. altitude profile obtained as for Figure 4 except that data division is according to a 4-step disturbance index which characterizes the state of agitation of a full upleg or downleg portion of a pass.

those energy inputs which are known to affect the total background density. An implication of Figures 4 and 5 is that the waves probably do not correlate strongly with the types of parameters which are known to correlate with the total density and hence would produce a systematic shift among the various profiles.

We have also looked for correlations with certain of these parameters directly with the same general result. A few of these correlations will be shown below. Before presenting these results, certain restrictions arising from data base limitations must be pointed out. Because of the nature of the AE orbit with its relatively slow motion of perigee, and the fact that we are restricted to the period when AE was in an elliptic orbit, there are cross couplings among the various parameters used. Some of these can be seen by examining Figure 6. For example, AE-C only samples latitudes close to the equator during the period July to September. In addition, our data coverage throughout the elliptic period is not uniform. Due to a combination of circumstances not all of the data taken during this time is available to us. As an engineering instrument, we do not have easy access to the AE central computer and so we have to depend on data being sent to us on tape; unfortunately, not all of the data is available in this form. Coverage is best between about orbit 2000 and orbit 3600 with some short periods scattered at other times. The results of the subsequent correlations should be viewed with this caveat in mind.

Correlations of wave activity with local time are shown in Figure 7. We are concerned here primarily with the two higher classifications (index numbers 3 and 4) where the wave structure is well defined and easily seen. Under these circumstances there may be a weak correlation with greater probability of these waves occurring late at night and in the evening. In Figure 8 we show a similar analysis using geographic latitude. In this case the correlation begins to show certain regularities. There are very few waves seen in higher northern latitudes (40° - 68° N). There are also relatively few seen near the equator. The regions of highest occurrence appear at relatively high southern latitudes (40° - 68° S) and centered at approximately 25° in both the Southern and Northern Hemispheres.

In Figure 9 the data have been divided into bins 10° wide in latitude and 30° wide in longitude. The shading shows the probability of encountering wave structure of either classification 3 or 4 within each bin. Because of the relatively large bin size, some of the finer scale features should not be taken too literally. The general characteristics of

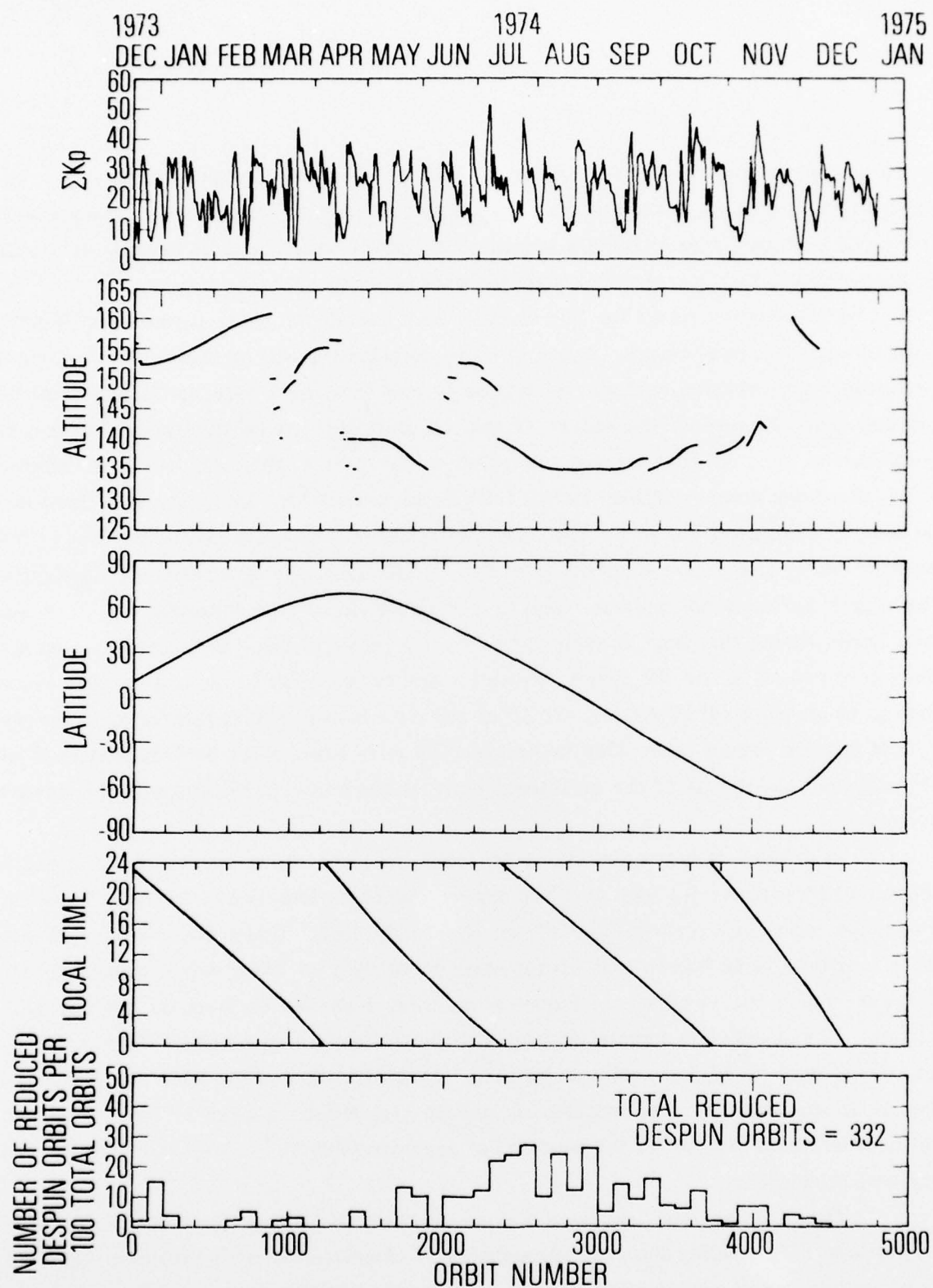


Figure 6.

Orbital parameters for AE-C encompassing the period of operation in the elliptic phase. The Kp values during this period and the relative orbit coverage within the reduced data base are also shown.

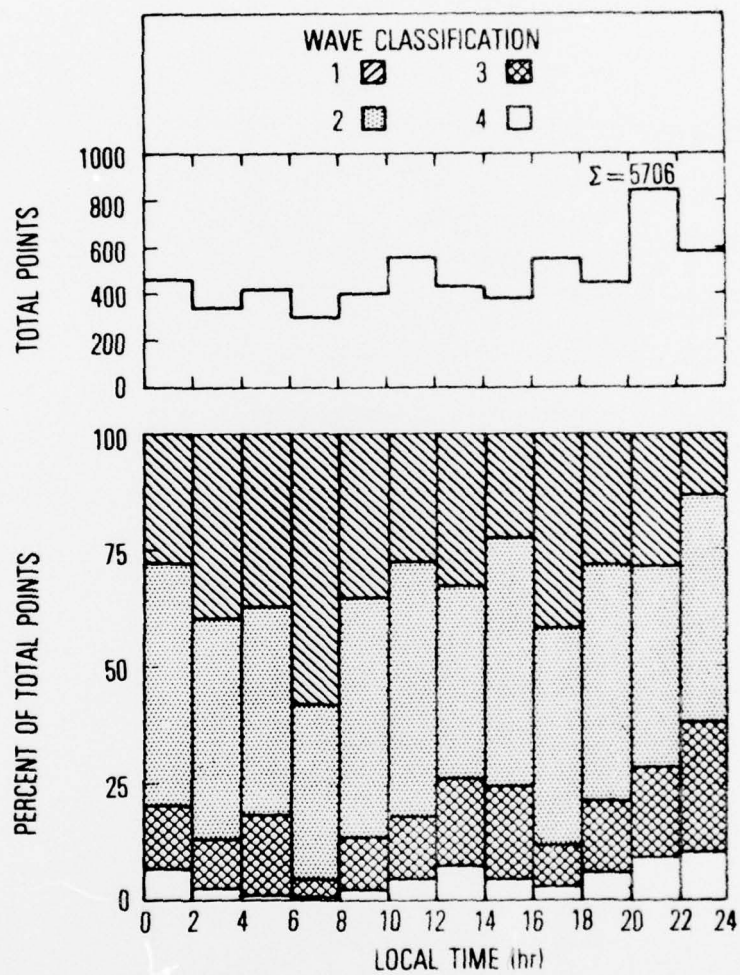


Figure 7. Percentage frequency of occurrence of each wave classification as a function of local time.

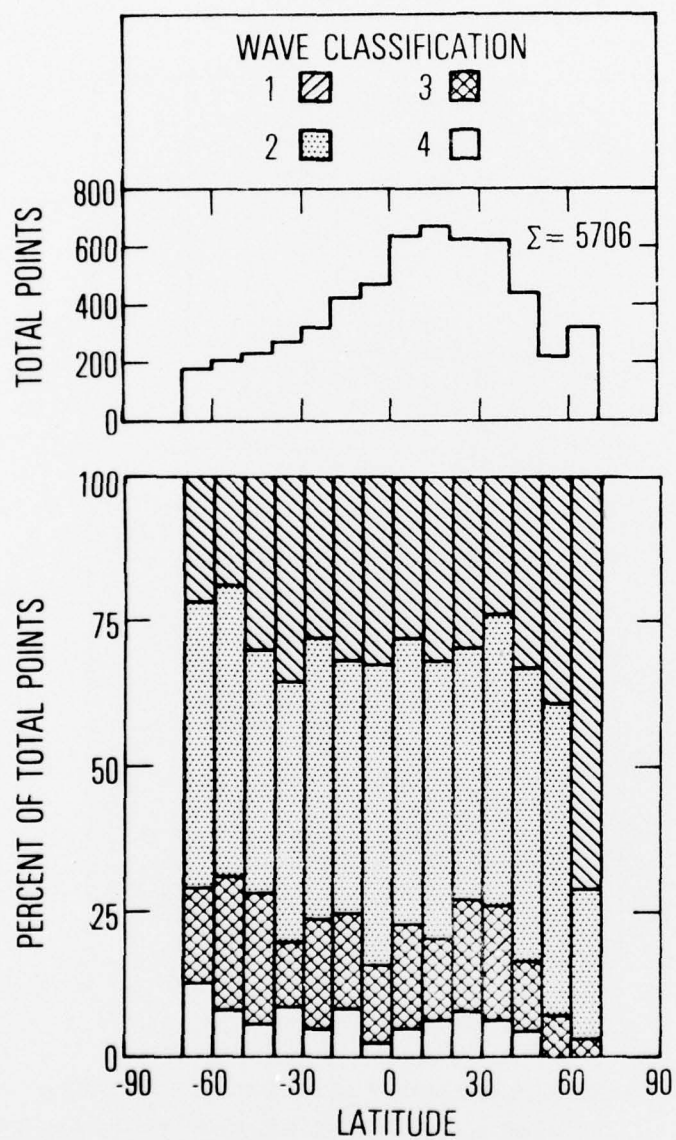


Figure 8. Percentage frequency of occurrence of each wave classification as a function of geographic latitude.

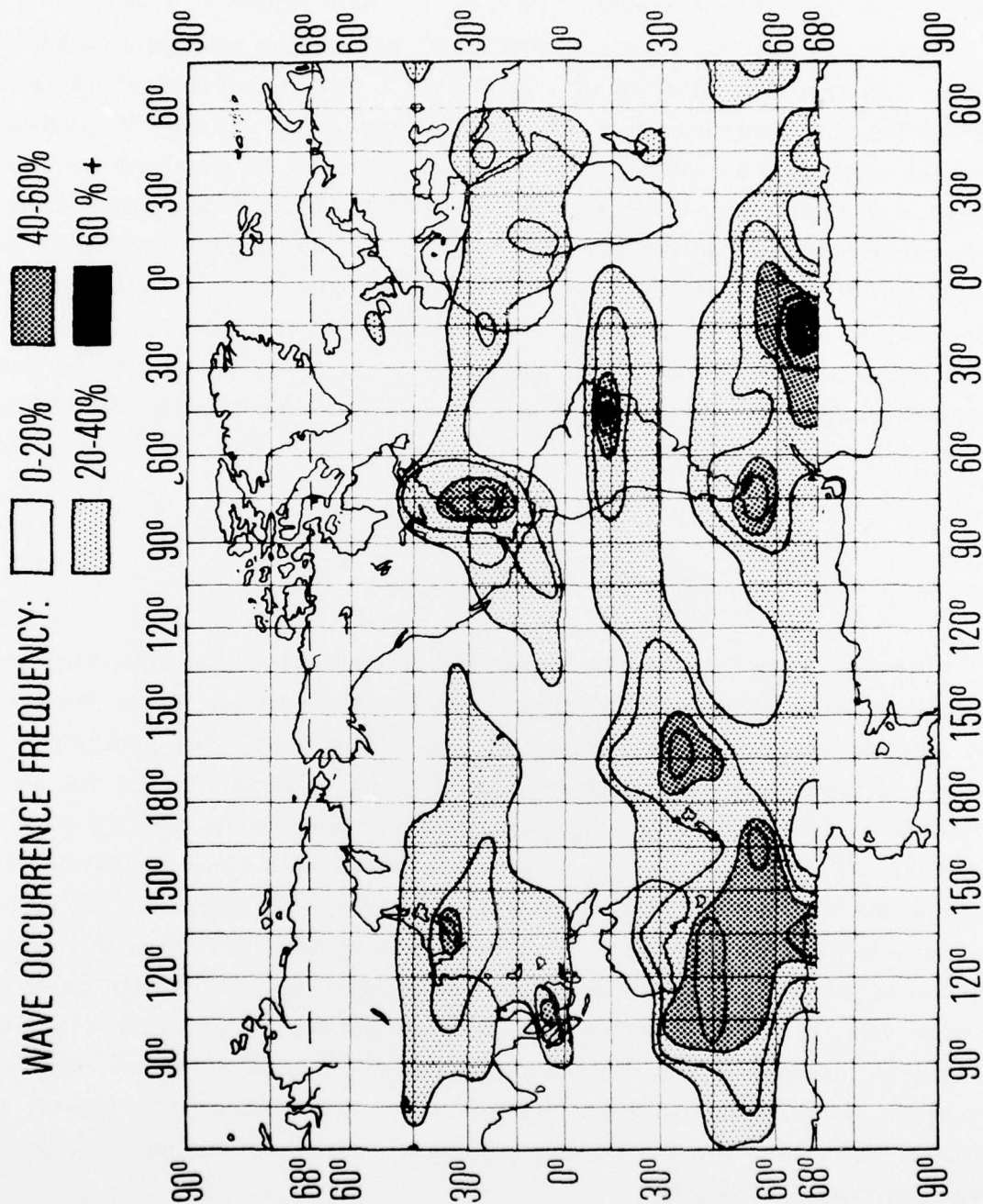


Figure 9. Contours showing percentage frequency of occurrence of wave classifications 3 and 4 as a function of latitude (10° bins) and longitude (30° bins).

the latitude structure pointed out earlier are evident in Figure 9 as well, but, in addition, there are some striking regularities in the longitudinal structure. With the exception of the belt of high activity surrounding Antarctica, the main regions of wave occurrence tend to fall just off the east coasts of continental land masses, principally in middle-latitudes. We have also split the data in half by a random selection of orbits and performed the same analysis on each half; the results are shown in Figure 10. Although differences, probably of a statistical nature, exist among them, the same basic structures reappear in all three maps. This technique for dividing the data assures that a single very disturbed orbit will not dominate both plots; it does not prevent a relatively long lived but nevertheless randomly located disturbance region from appearing in both. Elimination of this type of coupling requires a totally independent data base well removed in time; this technique for data division is precluded by the AE orbit characteristics (see Figure 6) but will be implemented as our AE-D and AE-E data bases expand.

DISCUSSION

If we confine our attention for the moment to the Northern Hemisphere in Figure 9, we find regions of high probability for wave structure along the east coasts of Asia and North America and over northern Africa and the middle east. This configuration is suggestive of the sub-tropical jet stream, which is shown in Figure 11. The data shown (Krishnamurti, 1961) give the average streamline and isotachs for the 200-mb level (approximately 12 km, near the top of the troposphere) for the winter of 1955-56. The three so-called "jet streaks", or regions where the wind velocity maximizes, are located in the same areas noted in connection with the thermospheric wave data of Figure 9. The three-wave pattern in the streamline exhibits considerable stability from day to day and from year to year. Furthermore, it is known that tropospheric and lower stratospheric convergence and divergence are associated with waves and regions of strong winds, in particular with jet streams. As a consequence, the areas off the continental east coasts are the primary regions of both cyclo- and anticyclo-genesis (Palmen and Newton, 1969).

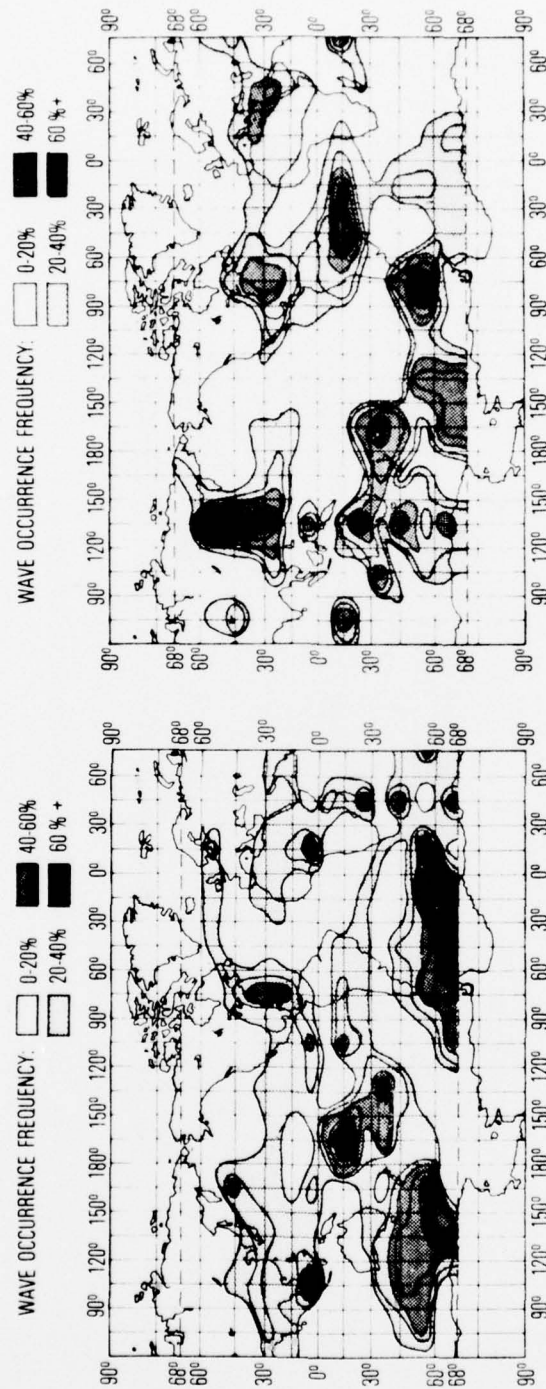


Figure 10. Same as Figure 9 except that data base has been divided into halves by a random selection of orbits.

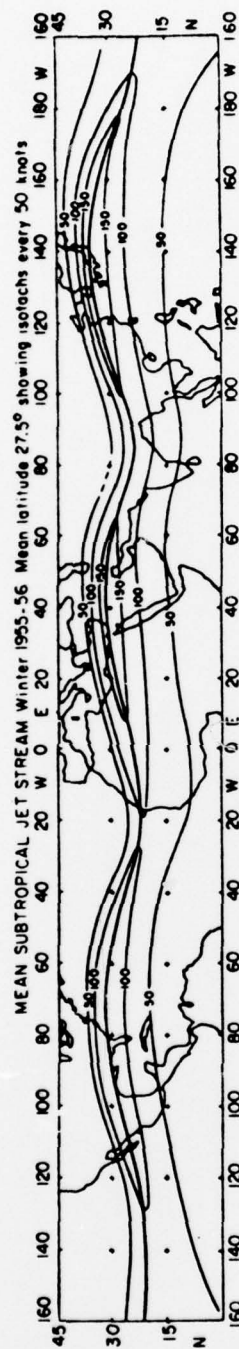


Figure 11.

Location of the mean sub-tropical jet stream during the winter of 1955-56. Isotachs are drawn for 50-knot intervals. The heavy continuous line in the center of a flow streamline following the maximum wind velocity. (Taken from Kirshnamurti, 1961.)

Investigators studying ground-level microbarograph records have been able to correlate very small periodic pressure fluctuations with wind shears and jet streams (Reed and Hardy, 1972, and Hooke and Hardy, 1975). It was theoretically suggested by Hines (1960) and confirmed by later authors (e.g., Gossard, 1962) that gravity waves generated in the troposphere could, under certain conditions, propagate into the thermosphere. This is evidently what is being seen here in the neutral density data.

Although upper tropospheric wind data are not as firmly established in the Southern Hemisphere as in the Northern, the available knowledge tends to support the correlation with thermospheric waves. Van Loon (1964) has published profiles of mid-season average zonal winds in the Northern and Southern Hemispheres. These data, reproduced in Figure 12, are for the 500-mb level, which is somewhat below the region of maximum winds which appears near 200 mb, but the general features are similar. Three things are worth pointing out: the Southern Hemisphere has higher velocity winds than the Northern Hemisphere at the same season; there is less seasonal variation in the south; and the peak velocity in the Southern Hemisphere is generally at a higher latitude than the peak in the Northern Hemisphere. Equating wind velocity (or possibly wind shear) with the probability of encountering thermospheric wave structure, we see similar characteristics in Figure 8 (except for seasonal variations, about which little can be said at the moment).

Average zonal winds at the 200-mb level for January and July are shown in Figure 13 (redrawn from Heastie and Stephenson, 1960). For comparison with our wind data in Figure 9, the most appropriate map is that for July. The principal wind maxima in the Southern Hemisphere are located over the South Indian Ocean and over Australia; in addition, the regions of high winds are more extended than in the Northern Hemisphere. Similar statements apply also to the thermospheric wind data in Figure 9. The only major discrepancy occurs in the wave data over South America; the maximum observed there may, however, be produced by particles precipitating in the South Atlantic anomaly.

In conclusion, we have demonstrated an apparent correlation between the appearance of wavelike structures in the neutral density in the lower thermosphere and the location of strong tropospheric winds. This correlation and theoretical considerations advanced by others (for example, Mastrantonio et al., 1976) suggest that the tropospheric wind systems are generating most of the internal gravity waves which subsequently propagate upwards into the thermosphere.

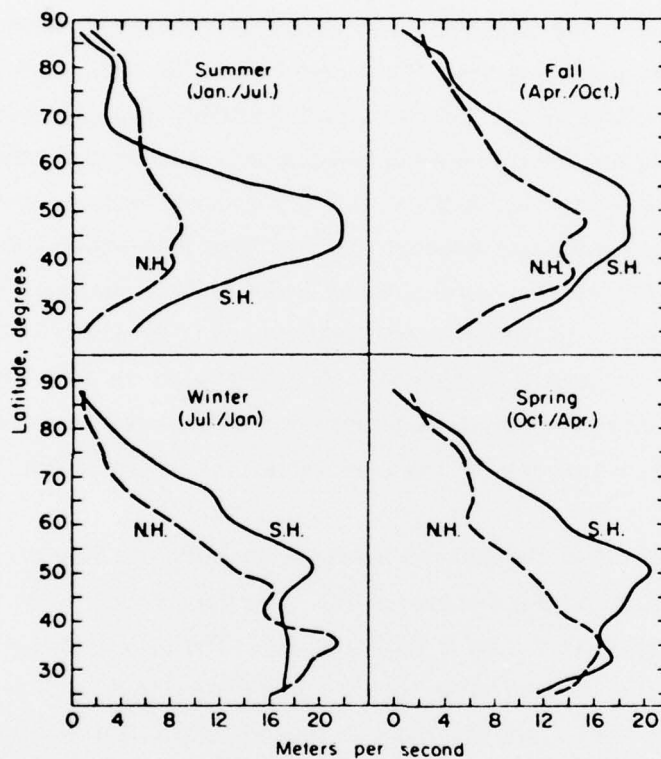


Figure 12. Profiles of average mid-season zonal winds at 500 mb in the Northern and Southern Hemispheres. The months given in parentheses are for the Southern/Northern Hemispheres, respectively. (Taken from Van Loon, 1964.)

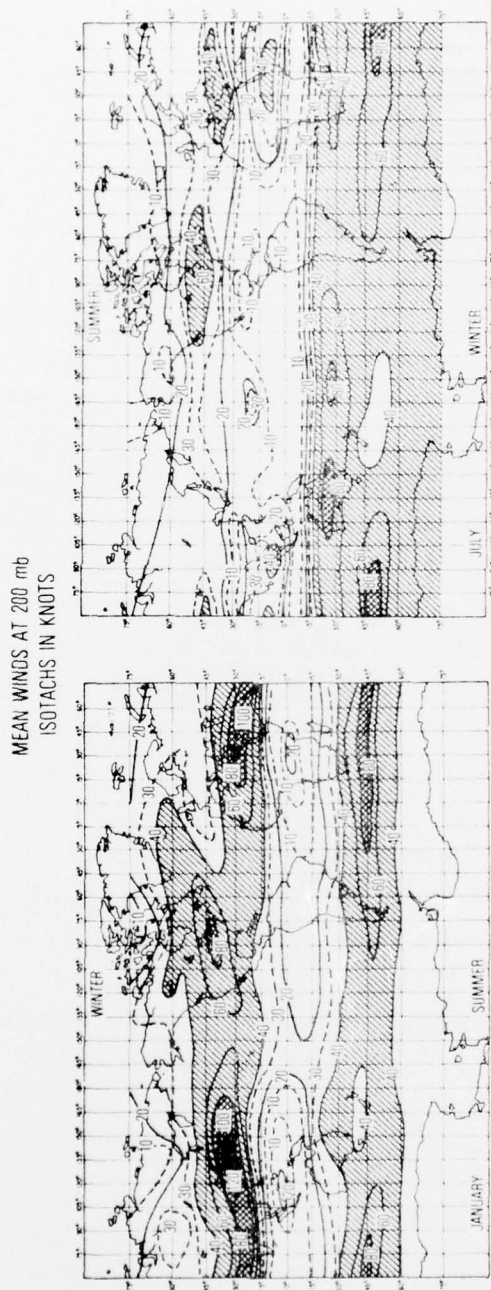


Figure 13. Mean winds at 200 mb in (a) January and (b) July. Contours are labeled in knots. (Redrawn from Heastie and Stephenson, 1960, by permission of the Controller, Her Britannic Majesty's Stationary Office.)

REFERENCES

CIRA, COSPAR International Reference Atmosphere 1965, North-Holland Publication Company, Amsterdam, 1965.

CIRA, COSPAR International Reference Atmosphere 1972, Akademie-Verlag, Berlin 1972.

Gossard, E.E., Vertical flux of energy into the lower ionosphere from internal gravity waves generated in the troposphere, J. Geophys. Res., 67, 745, 1962.

Heastie, H., and P.M. Stephenson, Upper winds over the world, parts I and II, Geophys. Mem. 23, No. 103, 1, 1960.

Hedin, A. E., H. G. Mayr, C. A. Reber, N. W. Spencer, and G. R. Carignan, Empirical model of global thermospheric temperature and composition based on data from the OGO-6 quadrupole mass spectrometer, J. Geophys. Res., 79, 215, 1974.

Hedin, A. E., J. E. Salah, J. V. Evans, C. A. Reber, G. P. Newton, N. W. Spencer, D. E. Kayser, D. Alcayde, P. Bauer, L. Cogger, and J. P. McClure, A global thermospheric model based on mass spectrometer and incoherent scatter data: MSIS, part 1-N₂ density and temperature, submitted to J. Geophys. Res. 1977a.

Hedin, A. E., C. A. Reber, G. P. Newton, N. W. Spencer, H. C. Brinton, H. G. Mayr, and W. E. Potter, A global thermospheric model based on mass spectrometer and incoherent scatter data: MSIS, part 2 - composition, submitted to J. Geophys. Res. 1977b.

Hines, C.O., Internal atmospheric gravity waves at ionospheric heights, Can. J. Phys., 38, 1441, 1960.

Hooke, W.H., and K.R. Hardy, Further study of the atmospheric gravity waves over the Eastern Seaboard on 18 May 1969, J. Appl. Meteorol., 14, 31, 1975.

Krishnamurti, T.N., The subtropical jet stream of winter, J. Meteorol., 18, 172, 1961.

Mastrantonio, G., F. Einaudi, D. Fua, and D.P. Lalas, Generation of gravity waves by jet streams in the atmosphere, J. Atmos. Sci., 33, 1730, 1976.

Palmen, E., and C.W. Newton, Atmospheric Circulation Systems, Academic Press, New York, 1969.

Reed, R.J., and K.R. Hardy, A case study of persistent, intense, clear air turbulence in an upper level frontal zone, J. Appl. Meteorol., 11, 541, 1972.

Rice, C. J., V. L. Carter, S. R. LaValle, W. T. Chater, D. A. Jones, C. G. King, and D. F. Nelson, Atmosphere explorer pressure measurements: ion gauge and capacitance manometer, Radio Sci., 8, 305, 1973.

Van Loon, H. , Mid-season average zonal winds at sea level and at 500 mb south of 25° south, and a brief comparison with the Northern Hemisphere, J. Appl. Meteorol. , 3, 554.

THE IVAN A. GETTING LABORATORIES

The Laboratory Operations of The Aerospace Corporation is conducting experimental and theoretical investigations necessary for the evaluation and application of scientific advances to new military concepts and systems. Versatility and flexibility have been developed to a high degree by the laboratory personnel in dealing with the many problems encountered in the nation's rapidly developing space and missile systems. Expertise in the latest scientific developments is vital to the accomplishment of tasks related to these problems. The laboratories that contribute to this research are:

Aerophysics Laboratory: Launch and reentry aerodynamics, heat transfer, reentry physics, chemical kinetics, structural mechanics, flight dynamics, atmospheric pollution, and high-power gas lasers.

Chemistry and Physics Laboratory: Atmospheric reactions and atmospheric optics, chemical reactions in polluted atmospheres, chemical reactions of excited species in rocket plumes, chemical thermodynamics, plasma and laser-induced reactions, laser chemistry, propulsion chemistry, space vacuum and radiation effects on materials, lubrication and surface phenomena, photo-sensitive materials and sensors, high precision laser ranging, and the application of physics and chemistry to problems of law enforcement and biomedicine.

Electronics Research Laboratory: Electromagnetic theory, devices, and propagation phenomena, including plasma electromagnetics; quantum electronics, lasers, and electro-optics; communication sciences, applied electronics, semiconducting, superconducting, and crystal device physics, optical and acoustical imaging; atmospheric pollution; millimeter wave and far-infrared technology.

Materials Sciences Laboratory: Development of new materials; metal matrix composites and new forms of carbon; test and evaluation of graphite and ceramics in reentry; spacecraft materials and electronic components in nuclear weapons environment; application of fracture mechanics to stress corrosion and fatigue-induced fractures in structural metals.

Space Sciences Laboratory: Atmospheric and ionospheric physics, radiation from the atmosphere, density and composition of the atmosphere, aurorae and airglow; magnetospheric physics, cosmic rays, generation and propagation of plasma waves in the magnetosphere; solar physics, studies of solar magnetic fields; space astronomy, x-ray astronomy; the effects of nuclear explosions, magnetic storms, and solar activity on the earth's atmosphere, ionosphere, and magnetosphere; the effects of optical, electromagnetic, and particulate radiations in space on space systems.

THE AEROSPACE CORPORATION
El Segundo, California

• • •